Int. J. Electrochem. Sci., 17 **(2022)** Article Number: 220657, doi: 10.20964/2022.06.60

International Journal of
ELECTROCHEMICAL
SCIENCE
www.electrochemsci.org

Short Communication

Enhanced Electrochemical Properties of $LiMn_2O_4$ Cathode Materials by Coating with ZnO

Guangfu Liu[1], *Shihang Dai*[2], *Qing Han*[1,*], *Kuiren Liu*[1]

[1] School of Metallurgy, Northeastern University, Shenyang 110819, PR China
[2] Shenyang Ligong University, Shenyang 110159, Liaoning Province, P. R. China
[*]E-mail: hanq@smm.neu.edu.cn

Received: 31 January 2022 / *Accepted:* 21 March 2022 / *Published:* 7 May 2022

$LiMn_2O_4$ cathode material is a potential cathode material for lithium ion battery. But poorly conductivity and magnification limit its widely application. Surface coating modification is an effective methord to raise the electrochemical performance of $LiMn_2O_4$. In this paper, ZnO coated $LiMn_2O_4$ to prepare modified $LiMn_2O_4$ material was prepared. The influence of ZnO coated $LiMn_2O_4$ material on the electrochemical properties was investigated. The results shown that LMO@Z exhibited better electrochemical properties than LMO. The initial discharge capacities of LMO@Z was 103.4 $mAh \cdot g^{-1}$ at 0.2 C-rate, After 100 cycles, the specific capacities of LMO@Z was 89.7 $mAh \cdot g^{-1}$with the capacity retention of 87.1%, whereas those of LMO only 60.6 $mAh \cdot g^{-1}$ with the capacity retention of 62.3%. It indicates that ZnO coated $LiMn_2O_4$ material could improve the electrochemical performance of $LiMn_2O_4$.

Keywords: $LiMn_2O_4$; ZnO; Coating; Electrochemical performance

1. INTRODUCTION

Lithium-ion batteries (LIBs) have been widely used in many fields because of theirs advantages such as high energy, long service life, low consumption, less pollution and no memory effect [1,2]. It is generally acknowledged that the performance of cathode material directly affects the performance of lithium battery, therefore the major research fields of lithium-ion battery concentrated on cathode material [3,4]. In recent years, cathode materials for massive commercial applications contain $LiNi_xCo_yMn_{1-x-y}O_2$ [5], $LiCoO_2$ [6], $LiFePO_4$ [7] and $LiMn_2O_4$ [8].

Among all the cathode materials for Lithium-ion battery, spinel $LiMn_2O_4$ has better application prospects since it's available of raw material, low price, safety, high discharge platform voltage and good room temperature cycle performance [9-11]. However, the poorly conductivity and magnification of spinel $LiMn_2O_4$ seriously influences its widely application [12]. To solve this problems, researchers used

different methods to modify lithium manganate which mainly consist of doping [13,14] and coating modification [15].

Surface coating modification is defined as achieving the purpose of preventing corrosion by coating a layer of material on the surface of $LiMn_2O_4$ [15]. Consequently, it can reduce the erosion of electrolyte on the surface of it, inhibit the dissolution of the surface, maintain the stability of the structure, and eventually improve the cycle performance. Normally, the metal oxides coating the surface of $LiMn_2O_4$ include metal oxides (such as Al_2O_3, TiO_2) [16,17], polymers [18], fluorides [19,20], conductive carbon [15], etc. Metal oxides are generally used for the coating of $LiMn_2O_4$ cathode materials. Especially ZnO was regarded as a desirable surface-coating material due to its excellent chemical and thermal stability. ZnO as surface-coating material using different coating techniques to improve their electrochemical performance [21].

The cycle performance of $LiMn_2O_4$ can be improved through coating with metal oxide on the surface of $LiMn_2O_4$, the reason is that, a spinel-like structure solid solution can be formed on the surface of $LiMn_2O_4$, the direct contact between the electrolyte and the electrode surface can be reduced. The dissolution of Mn can be greatly inhibited as the reaction between oxide and HF [15,16].

In this paper, bare $LiMn_2O_4$ was synthesized by precipitation method, and ZnO coated $LiMn_2O_4$ to prepare modified $LiMn_2O_4$ material. The influence of ZnO coated $LiMn_2O_4$ material on the electrochemical properties was investigated. Results showed that ZnO coated $LiMn_2O_4$ material could improve the electrochemical performance of $LiMn_2O_4$.

2. EXPERIMENTAL

2.1 Material preparation

Lithium carbonate (Li_2CO_3, AR, 99.9%), Manganese acetate ($C_4H_6MnO_4{\cdot}4H_2O$, AR), Sodium oxalate ($Na_2C_2O_4$), and Zinc acetate dihydrate ($C_4H_6O_4Zn{\cdot}2H_2O$) were used as raw materials. All the regents used are of analytical grade.

2.1.1. Prepare of $LiMn_2O_4$

The molar ratio of $C_4H_6MnO_4{\cdot}4H_2O$ to $Na_2C_2O_4$ was 1:1.25. First, 2.451 g $C_4H_6MnO_4{\cdot}4H_2O$ was dispersed in 100 mL deionized water, 1.675 g $Na_2C_2O_4$ was dispersed in 100 mL deionized water, and $Na_2C_2O_4$ solution was added to the stirring $C_4H_6MnO_4$ solution in drops. After stirring for 1 h, the obtained MnC2O4 was filtered, washed, and dried at 100 °C over night; 0.381 g Li_2CO_3 and MnC2O4 were ground and mixed with a mortar to obtain the precursor of $LiMn_2O_4$; The precursor was calcined at 500° C for 3 h, then heated to 720° C in air for 15 h, after cooling to room temperature. The resulting powder is bare $LiMn_2O4$ (termed as LMO).

2.1.2. Preparation of $LiMn_2O_4$/ZnO

0.027 g $C_4H_6O_4Zn{\cdot}2H_2O$ was dispersed in 30 mL ethyl alcohol, 0.5 g LMO was add in the ethanol solution. Under water bath conditions at 80 °C to volatilize ethyl alcohol. The obtained powder was put into a muffle furnace and then heated to 600 °C for 2 h in air to prepare $LiMn_2O_4$/ZnO (termed as LMO@Z). The schematic diagram of the preparation of LiMn2O4/ZnO is shown in Figure 1.

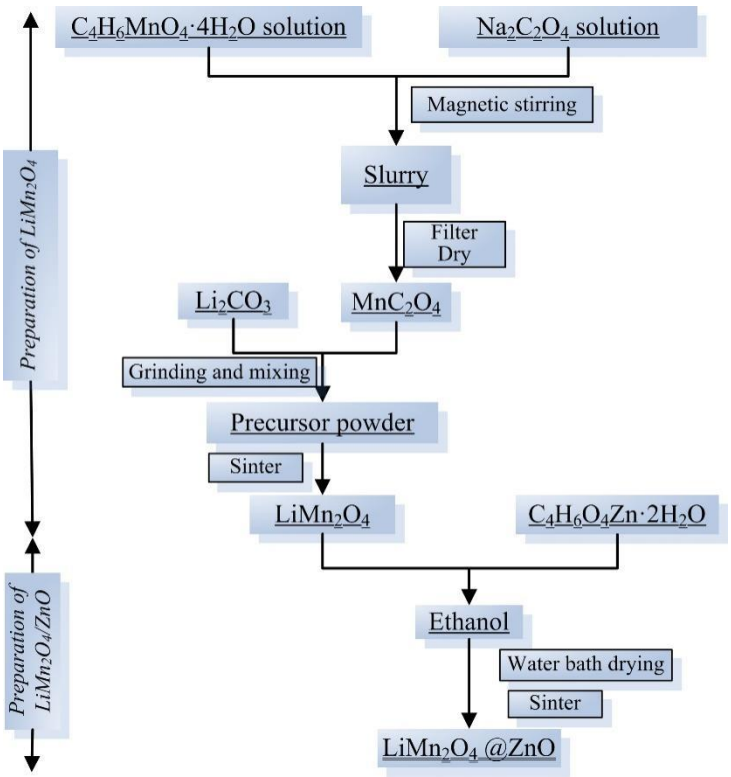

Figure 1. Schematic illustration of preparation $LiMn_2O_4$@ZnO.

2.2. Materials characterization and electrochemical measurement

X-ray powder diffraction (XRD, Shimadzu 6100) was applied to determined the crystal structure of the as-synthesized powders. Scanning electron microscope (SEM, Zeiss sigma300) was used to analyzed the microstructures of the as-synthesized powders.

The as-synthesized powders mixed with acetylene black and polyethylene difluoride (PVDF) at a weight ratio of 80:10:10 to fabricate the electrodes. The mixture was added in NMP stirring for 8 h to form an electrode slurry. The slurry was heated at 100 °C for 10 h under vacuum after coated on an aluminum foil. Li foils, 1 M $LiPF_6$-EC:DMC:EMC=1:1:1 vol% and Celgard 2300 films were used as anode electrode, electrolyte and separator, respectively.

The electrochemical properties of the as-synthesized powders were tested using CR2032 coin cells.Cycle charge-discharge behavior of the cells were performed with Battery-testing system (Neware Co., Ltd., China) between 3.3-4.5V (vs Li/Li^+). Electrochemical impedance spectroscopy (EIS)

measurements (0.1-100 kHz) and Cyclic voltammetry (CV) test (3.3-4.5V, 0.3 $mV \cdot s^{-1}$) were both performed with electrochemical work-station (CHI660E).

3. RESULTS AND DISCUSSION

Figure 2(a) shows the XRD patterns of LMO and LMO@Z samples. All the diffraction peaks of the two samples revealed at 18.6°, 36.2°, 37.9°, 44.0°, 48.1°, 58.2°, 63.9° and 67.3°, which were indexed to the (111), (311), (222), (400), (311), (511), (440) and (531) crystal planes of spinel $LiMn_2O_4$ (JCPDS: 35-0782) with the Fd-3m space group [22]. All the peaks of LMO and LMO@Z were agreement with spinel structure without any diffraction peak of impurity.It indicating that ZnO coated $LiMn_2O_4$ did not significantly affect the spinel structure of $LiMn_2O_4$.

Rietveld analysis of XRD patterns of LMO and LMO@Z samples are shown in Fig 2(b) and Fig 2(c). The lattice parameters of as-synthesized samples are shown in Table 1. LMO@Z exhibited greater the crystal parameters and cell volume than those of LMO, big cell volume can supply rapid ion channels which is conducive to the diffusion of Li-ions [23].

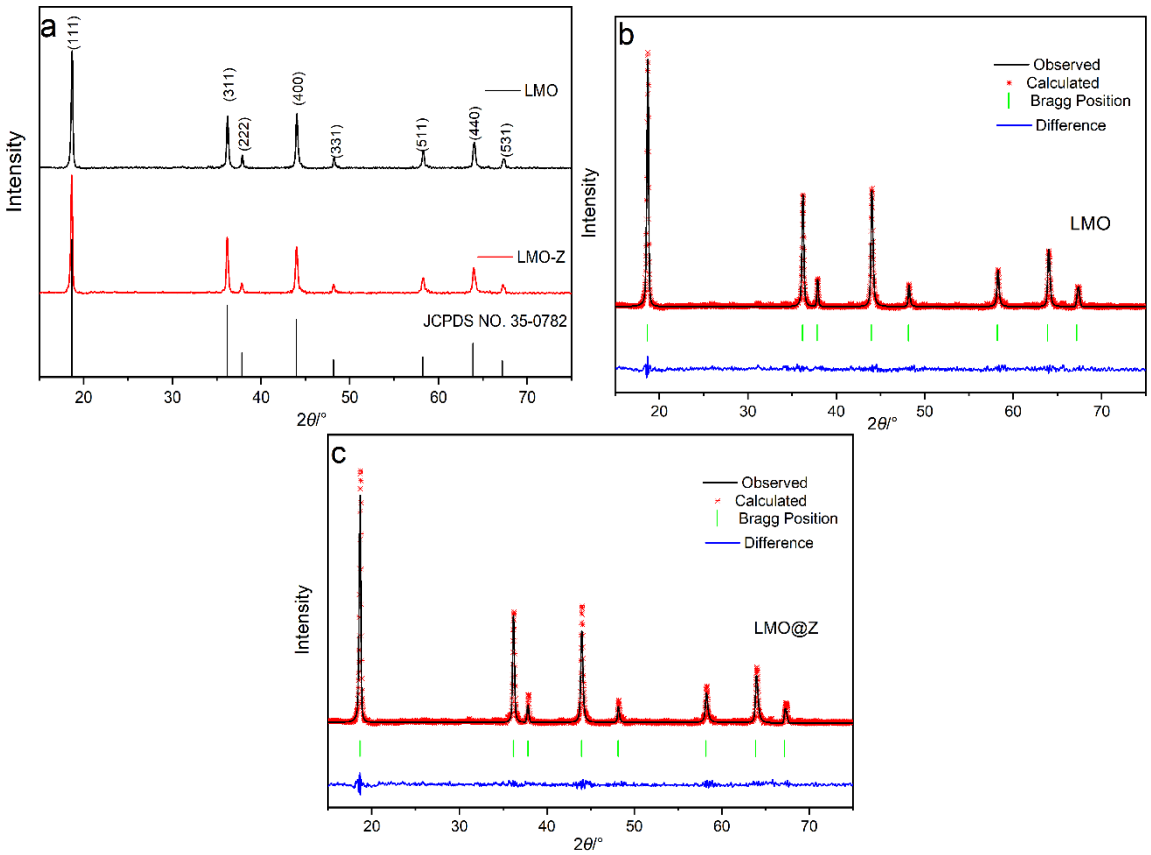

Figure 2. (a) XRD patterns and the corresponding Rietveld refinement of (b) LMO and (c) LMO@Z.

Table 1. Crystalline parameters of LMO and LMO@Z

Samples	*a*(Å)	*b*(Å)	*c*(Å)	V(Å^3)
LMO	8.2218	8.2218	8.2218	555.78
LMO@Z	8.2282	8.2282	8.2282	557.09

Figure 3 shows the SEM images of LMO and LMO@Z. The particles in LMO were uniformly distributed with the size mainly around 0.2-0.8 μm. While most of the particles in LMO@Z were most fluffy and fine particles with the size mainly around 0.2-0.5 μm, and some large particles were built up by numerous small particles with the size about 0.2 μm. Small particles can shorten transmission paths of Li-ions, which is conducive to the improvement of charge and discharge performance [24].

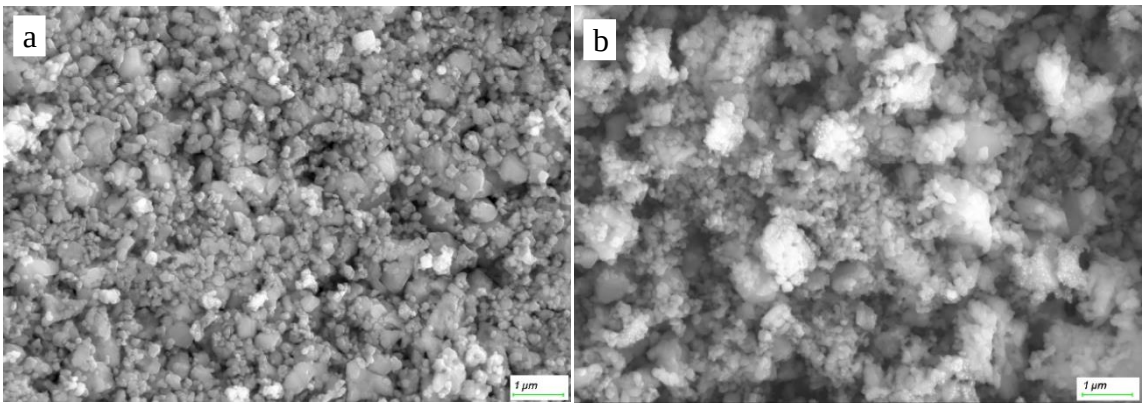

Figure 3. SEM images of (a) LMO and (b) LMO@Z.

Figure 4 (a), (b) and (c) show the initial specific capacity-potential curves, cycling performance at 0.2 C-rate and 1.0 C-rate of LMO and LMO@Z. The charge-discharge curves of LMO and LMO@Z all had two voltage plateaus, which were agreement with that lithium ions intercalation and delamination in $LiMn_2O_4$ were carried out in two steps [25,26]. The initial specific capacity of LMO was 97.2 mAh·g^{-1} with the coulombic efficiencies of 93.3%, while that of LMO@Z was 103.4 mAh·g^{-1} with the coulombic efficiencies of 94.5%. Compared with LMO, LMO@Z exhibited a higher initial specific capacity.

After 100 cycles at 0.2 C-rate, the specific capacities of LMO and LMO@Z were 60.6 and 89.7 mAh·g^{-1} with the capacity retentions of 62.3% and 87.1%, respectively. It shown that LMO@Z exhibited a better electrochemical performance.

After 100 cycles at 1.0 C-rate, the specific capacities of LMO and LMO@Z were 47.5 and 76.5 mAh·g^{-1} with the capacity retentions of 58.9% and 86.2%, respectively. It also shown that LMO@Z exhibited a better electrochemical performance.

Figure 4 (d) shows the discharge rate capacities carried out from 0.1 to 5.0 C of LMO and LMO@Z. The discharge capacity decreases from 97.2 mAh·g^{-1} at 0.2 C to 91.0 mAh·g^{-1} at 0.5 C, 80.9 at 1.0 C, 71.5 mAh·g^{-1} at 2.0 C, 60.7 mAh·g^{-1} at 5.0 C, and then to 89.2 mAh·g^{-1} current rate return back

to 0.2 C again, with recovery rate of 91.7% for LMO; while the discharge capacity decreases from 103.4 $mAh \cdot g^{-1}$ at 0.2 C to 96.8 $mAh \cdot g^{-1}$ at 0.5 C, 88.1 at 1.0 C, 81.6 $mAh \cdot g^{-1}$ at 2.0 C, 70.1 $mAh \cdot g^{-1}$ at 5.0 C, and then to 99.1 $mAh \cdot g^{-1}$ current rate return back to 0.2 C again, with recovery rate of 95.8% for LMO@Z. Thus,LMO@Z had a better rate performance than that of LMO.

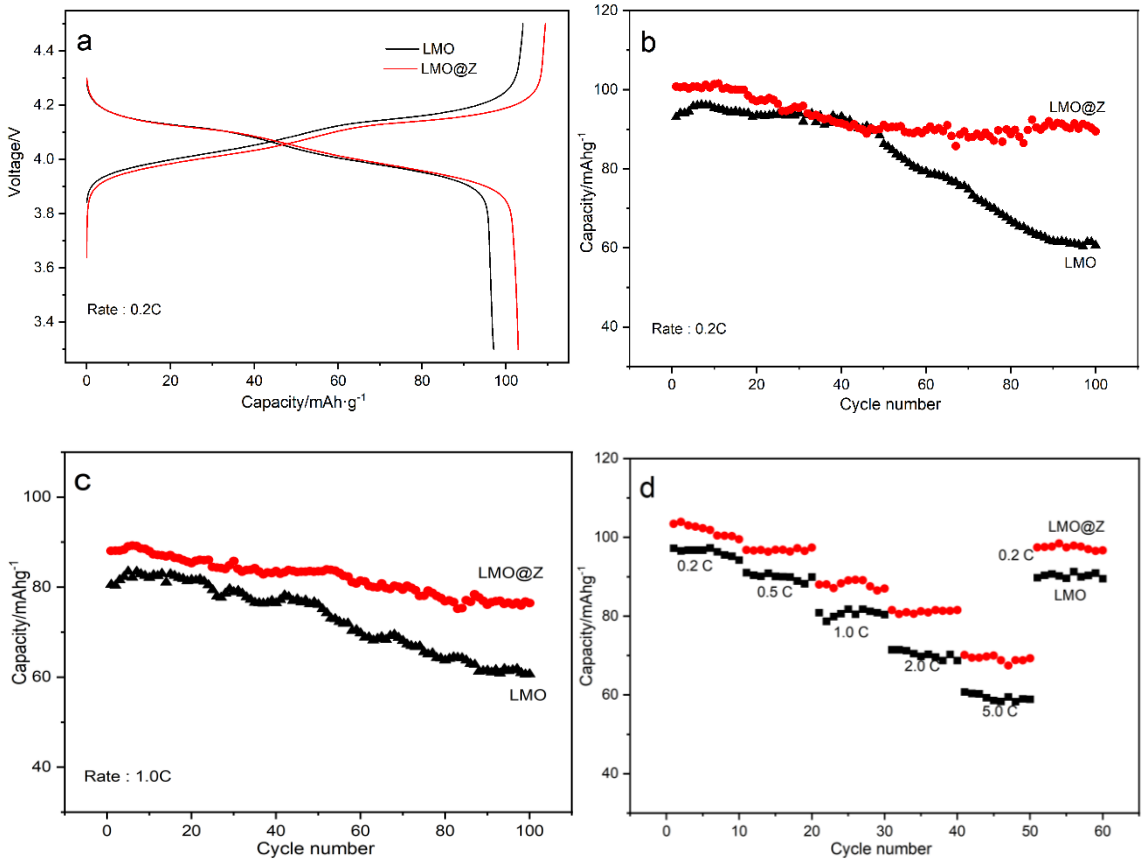

Figure 4. (a) Initial specific capacity-potential curves; (b) cycling performance at 0.2 C-rate; (c) cycling performance at 1.0 C-rate; (d)rate performance of LMO and LMO@Z.

Compard with LMO, LMO@Z had a better electrochemical performance. It can explained by following reasons: first, LMO@Z exhibited greater the crystal parameters and cell volume than those of LMO, big cell volume can supply rapid ion channels which is conducive to the diffusion of Li-ions; Finally, ZnO coated on the surface of $LiMn_2O_4$, the direct contact between the electrolyte and the electrode surface can be reduced. Mn^{3+} dissolution can be cracked down on due to ZnO particles.

Figure 5(a) illustrated the cyclic voltammetry (CV) curves of LMO and LMO@Z. There were two pairs of redox peaks in the CV curves of both the samples, which were agreement with extraction/insertion of lithium ions [25,26]. The two pairs of redox peaks were consistent two plateaus of capacity-potential curves in Fig. 4 (a). The peak parameters of the CV curves is shown in Table 2.

In comparison, the separation (ΔE_p) between E_{pa} and E_{pc} were 267 and 180 mV for LMO, whereas those of LMO@Z were 200 and 135 mV, respectively. LMO@Z had smaller ΔE_p than those of LMO, which was indicated that LMO@Z had the faster intercalation/deintercalation process of Li^+ [27].

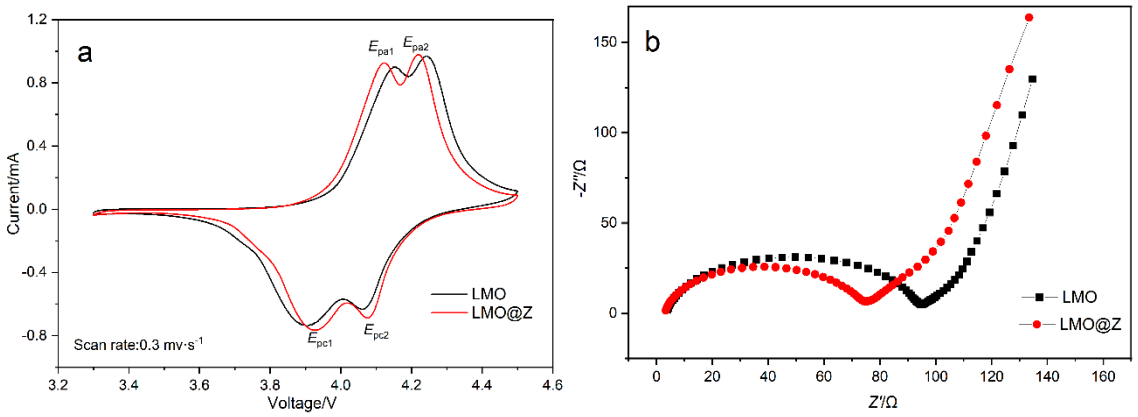

Figure 5. (a) CV curves and (b) Nyquist plots of LMO and LMO@Z.

Table 2. Peak parameters of CV curves for as-synthesized samples; $\Delta E_p = E_{pa} - E_{pc}$.

Sample	E_{pa1} (V)	E_{pa2} (V)	E_{pc1} (V)	E_{pc2} (V)	ΔE_{p1} (mV)	ΔE_{p2} (mV)
LMO	4.152	4.240	3.885	4.060	267	180
LMO@Z	4.123	4.213	3.923	4.078	200	135

Figure 5(b) shows the electrode reaction impedance (EIS) of as-synthesized samples before cycle. The impedance spectra of LMO and LMO@Z both had a semicircle in the high frequency region and a diagonal line in lower frequency region.

Table 3. The results of EIS of as-synthesized samples.

Sample	R_s/Ω	R_{ct}/Ω
LMO	3.8	94.9
LMO@Z	3.4	74.4

Table 3 exhibits the results of the EIS, the resistance of electrolyte (R_s) of LMO and LMO@Z were nearly the same. In comparison, the charge-transfer resistance (R_{ct}) of LMO was 94.9 Ω, whereas that of LMO@Z was 74.4 Ω. Compared with LMO, LMO@Z had a smaller charge-transfer resistance, indicating LMO@Z had a lower polarization. It is known that small R_{ct} is helpful to overcome the kinetic limitations during charge/discharge process, which can boost the diffusion of Li^+ [28].

Lithium manganate has been surface coating modification by many research groups and the related electrochemical data were summarized in Table 4. As shown in Table 4, surface coating modification is an effective way to improve electrochemical performance of lithium manganate.

Table 4. Comparison of lithium manganate were surface coating modification

LMO	Rate capacity ($mAhg^{-1}$)	LMO@X	Rate capacity ($mAhg^{-1}$)	References
LMO	80.9 (1.0 C); 71.5 (2.0 C); 60.7 (5.0 C)	LMO@ZnO	88.1 (1.0 C); 81.6 (2.0 C); 70.1 (5.0 C)	As prepared
LMO		LMO@Al_2O_3	87.4 (1.0 C); 70 (2.0 C); 60(5.0 C)	[29]
LMO	109.9 (1.0 C); 93.6(2.0 C); 80.7(5.0 C)	LMO@AlF_3	103.4(1.0 C); 94.8 (2.0 C); 89.1(5.0 C)	[30]

4. CONCLUSIONS

To sum up, the bare $LiMn_2O_4$ was synthesized by the precipitation method, and the modified $LiMn_2O_4$ material was obtained by coating the surface of $LiMn_2O_4$ with ZnO. The effect of ZnO-coated $LiMn_2O_4$ material on its properties was investigated. XRD results revealed that ZnO coated $LiMn_2O_4$ did not significantly affect the spinel structure of $LiMn_2O_4$; SEM studies confirmed LMO@Z had small primary particle size; electrochemical measurement results shown LMO@Z had better electrochemical properties than those of LMO. The results show that the ZnO-coated $LiMn_2O_4$ material can improve the electrochemical performance of $LiMn_2O_4$.

ACKNOWLEDGMENTS
This research did not receive any specific grant from funding agencies in the public, commercial, or not-for-profit sectors.

References

1. A. Pasquier, I. Plitz, S. Menocal and G. Amatucci, *J. Power Sources,* 11 5(2003) 171.
2. G. Mulder, N. Omar, S. Pauwels, M. Meeus, F. Leemans, B. Verbrugge, W.D. Nijs, P.V. Bossche,D. Six and J.V. Mierlo, *Electrochim. Acta,* 87 (2013) 473.
3. J.B. Goodenough and K.S. Park, *J. Am. Chem. Soc.*, 135 (2013) 1167.
4. N. Nitta, F. Wu, J.T. Lee and G. Yushin, *Mater. Today,* 18 (2015) 252.
5. Y. Yang, G. Huang, M. Xie, S. Xua and Y. He, *Hydrometallurgy,* 165 (2016) 358.
6. Z. Qu, S. Liu, P. Zhang, R. Wang, H. Wang, B. He, Y. Gong, J. Jin and S. Li, S*olid State Ionics,* 365 (2021) 115654.
7. W.J. Zhang, *J. Power Sources,* 196 (2011) 2962.
8. J.S. Ko, M.B. Sassin, D.R. Rolison and J.W. Long, *Electrochim. Acta,* 275 (2018) 225.
9. Y. Chen, Y. Tian, Y. Qiu, Z. Liu, H. He, B. Li and H. Cao, *Materials Today Advances*, 1 (2019) 1.
10. Y. Haijun and Z. Haoshen, *J. Phys. Chem. Lett.,* 4 (2013) 1268.
11. S. Huang, H. Wu, P. Chen, Y. Guo, B. Nie, B. Chen, H. Liu and Y. Zhang, *J. Mater. Chem. A,* 3 (2015) 3633.
12. J.S. Ko, M.B. Sassin, D.R. Rolison and J.W. Long, *Electrochim. Acta,* 275 (2018) 225.

13. K. Raju, F.P. Nkosi, E. Viswanathan, M.K. Mathe, K. Damodaran and K.I. Ozoemena, *Phys. Chem. Chem. Phys.*, 18 (2016) 13074.
14. S. Yang, D.O. Schmidt, A. Khetan, F. Schrader, S. Jakobi, M. Homberger, M. Noyong, A. Paulus, H. Kungl and R.A. Eichel, *Materials*, 11 (2018) 806.
15. Y. Chen, Y. Tian, Y. Qiu, Z. Liu, H. He, B. Li and H. Cao, *Materials Today Advances*, 1 (2019) 100001.
16. H. Wang, J. Han, L. Li, F. Peng, F. Zheng, D. Huang, F. Lai, S. Hu, Q. Pan and Q. Li, *J. Alloy Compd.*, 860 (2021) 158482.
17. K.W. Sung, D.Y. Shin and H.J. Ahn, *J. Alloy Compd.*, 870 (2021) 159404.
18. K.A. Vorobeva, S.N. Eliseeva, R.V. Apraksin, M.A. Kamenskii, E.G. Tolstopjatova and V.V.Kondratiev, *J. Alloy Compd.*, 766 (2018) 33.
19. T. Yeong, D. Park and J. Mun, *J. Power Sources*, 325 (2016) 360.
20. K. Park, J.H. Park, S.G. Hong, J. Yoon, S. Park, J.H. Kim, D. Yoon, H. Kim, Y.H. Son, J.H. Park and S. Kwon, *Electrochim. Acta*, 222 (2016) 830.
21. Q.L. Li, W.Q. Xu, H.L. Bai, J.M. Guo and C.W. Su, *Ionics* 22 (2016) 1343.
22. W. Zhang, X. Sun, Y. Tang, H. Xia, Y. Zeng, L. Qiao, Z. Zhu, Z. Lv, Y. Zhang, X. Ge, S. Xi, Z. Wang, Y. Du and X. Chen, *J. Am. Chem. Soc.*, 141 (2019) 14038.
23. L. Yao, Y. Xi, H. Han, W. Li, C. Wang and Y. Feng, *J. Alloy Compd.*, 868 (2021) 159222.
24. Y. Xue, Z.B. Wang, F.D. Yu, Y. Zhang and G.P. Yin, *J. Mater. Chem. A* 2 (2014) 4185.
25. E. Hosono, T. Kudo, I. Honma, H. Matsuda and H. Zhou, *Nano Lett.*, 9 (2009) 1045.
26. H.Y. Zhao, F. Li, X.Q. Liu, W.Q. Xiong, B. Chen, H.L. Shao, D.Y. Que, Z. Zhang and Y. Wu, *Electrochim. Acta*, 166 (2015) 124.
27. R.Y. Jiang, C.Y. Cui, H.Y. Ma, H.F. Ma and T. Chen, *J. Electroanal. Chem.*, 744 (2015) 69.
28. B. Han, X.D. Meng, L. Ma and J.Y. Nan, *Ceram. Int.*, 42 (2016) 2789.
29. H. Wang, J. Han, L. Li, F. Peng, F. Zheng, D. Huang, F. Lai, S. Hu, Q. Pan and Q. Li, *J. Alloy Compd.*, 860 (2021) 158482.
30. A. Tron, Y. D. Park and J. Mun, *J. Power Sources*, 325 (2016) 360.